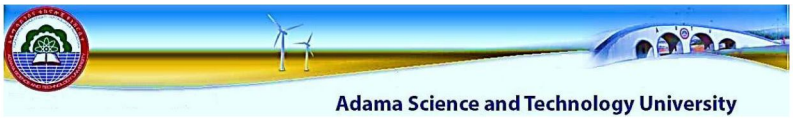

Effects of Impact Ionization on the Photo-response of a small and Direct Band-gap Bulk Semiconductor

By

Bayisa Amensisa Bulto

December 2016

Effects of Impact Ionization on the Photo-response of a small and Direct Band-gap Bulk Semiconductor

By

Bayisa Amensisa

Submitted in Partial fulfillment of the requirements for the degree of Master of Science in Physics (Material Science)
In the School of Applied Natural Science at Adama Science and Technology University

Advisor

Dr. Megersa Wodajo

December 2016

Adama, Ethiopia

ADAMA SCIENCE AND TECHNOLOGY UNIVERSITY
POSTGRADUATE PROGRAM
SCHOOL OF APPLIED NATURAL SCIENCE
APPLIED PHYSICS PROGRAM

As thesis research advisor, I hereby certify that I have read and evaluated this thesis entitled: **"Effects of Impact Ionization on the Photo-response of a small and Direct-Band-gap Bulk Semiconductor**" prepared under my guidance by Bayisa Amensisa. I recommend that it can be submitted as fulfilling the thesis requirement.

Dr. Megersa Wodajo	_____	_____
Advisor	Signature	Date

As members of the Board of Examiners of the M.Sc. thesis Open Defense Examination, we certify that we have read and evaluated the thesis work prepared by **Bayisa Amensisa** and examined the candidate. We recommended that the thesis be accepted as fulfilling the thesis requirement for the Degree of Master of Science in Physics.

_____	_____	_____
Chairperson	Signature	Date

_____	_____	_____
Internal Examiner	Signature	Date

_____	_____	_____
External Examiner	Signature	Date

Declaration and Statement of the Candidate

This thesis has been submitted in partial fulfillment of the requirements for M.Sc. degree at the ASTU. I solemnly declare that this thesis work is not submitted to any other institution anywhere for the award of any academic degree, diploma, or certificate.

Brief quotations from this thesis are allowable without special permission provided that accurate acknowledgement of source is made. Requests for permission for extended quotation from or reproduction of this manuscript in whole or in part may be granted by the head of major department or the Dean of the School of Graduate Studies when in his or her judgment the proposed use of the material is in the interests of scholarship. In all other instances, however, permission must be obtained from the author.

Name of candidate: Bayisa Amensisa Signature: _____

Place: Adama Science and Technology University, Adama

Date of Submission: December, 2016

Acknowledgements

First of all, I would like to start with my advisor Dr. Megersa Wodajo for his professional and endless support and patience, faithful and immense affection to help me from the beginning to the end of my study in the program of material science. Once again, I would like to express my sincere gratitude to him for his valuable guidance, inspiration, by giving some practical measured parameters and great material support throughout my entire thesis work. This work has been in its present shape with considerable professional and material inputs from various sources. Therefore, it is amazing excitement to me to come this final point and to express my deepest gratitude to all individuals and organizations who contributed directly or indirectly to this study thesis work.

Last but not least, my heartfelt gratitude goes to fellow friends and colleagues. They deserve special thanks for their valuable contributions and encouragement.

Contents

List of Figures

Figures **pages**

List of Abbreviations

E_F	Fermi energy (thermal equilibrium)
E_g	Energy band-gap of a semiconductor
E_i	Intrinsic Fermi energy
E_V	Valence band energy of a semiconductor
m_o	Free electron mass
m_e^*	Effective mass of electrons
m_h^*	Effective mass of holes
n	Electron density
n_i	Intrinsic carrier density
n_o	Electron density in thermal equilibrium
N_C	Effective density of states in the conduction band
N_a^-	Extrinsic density
Δn	Excess electron density
N_V	Effective density of states in the valence band
p	Hole density
p_o	Hole density in thermal equilibrium
Δp	Excess hole density
σ	Conductivity
τ_n	Electron lifetime
τ_p	Hole lifetime
τ_{eff}	Effective lifetime
C_R	Radiative Capture Coefficient
C_{pa}	Hole Auger Capture Coefficient
C_{na}	Electron Auger Capture Coefficient
k_B	Boltzmann's constant
TPV	Thermo-photovoltaic

Abstract

In this study, the effects of impact ionization and optical generation of carriers on the photo-response of gallium antimonide (GaSb) is described through the simulation of excess carrier lifetimes corresponding to the Auger and radiative recombination mechanisms using the relations describing the lifetimes of the excess minority carriers in the bulk of direct band gap semiconductor. First, the room temperature doping level dependence of excess carrier lifetimes related to the radiative and Auger recombination mechanisms and the combined effect of the two recombination mechanisms were described. Then, the temperature dependence of the excess carrier lifetimes was described using the simulation of the temperature dependence of the thermal equilibrium carrier concentration obtained using the Hall effect measurements for the samples with different doping levels along with the relations describing the lifetimes of the excess minority carriers in the bulk of direct band gap semiconductor. Finally, the room temperature injection level dependence of the steady state excess carrier lifetimes was described in samples with different doping levels by varying excess carrier's concentration from very low injection level to very high injection level. Since GaSb is a small and direct band gap semiconductor, all the intra-band transitions were neglected and only inter-band generation-recombination of free carriers was considered. The effective excess carrier lifetime for free carriers is in general found to be decreasing with increasing the doping level and the injection level of excess carriers. The radiative effect is found to be influential in the lower doping level regime and lower injection ranges of injection levels, while the impact ionization totally dominates the higher doping regime and higher injection level. Even though the impact ionization highly dominates the higher temperature region of the entire excess carrier lifetime, the variation in both the radiative and the Auger effect have no significant difference in the complete ionization region temperature region. The variation of the excess carrier lifetimes was intensified in the low temperature region due to freeze-out of charge carriers and at high temperature due to intrinsic effect. As the temperature increases, the excess carrier lifetime decreases, and the impact ionization totally dominates in the higher temperature regime. Because of the Auger and radiative recombination mechanisms are the reverse processes of the impact ionization and optical generation, respectively, the two reverse process are equal by the principle of the detailed balance.

Chapter 1

Introduction

Semiconductors are materials that are very important in modern optoelectronic technologies. The existence of the energy band gap, high density of charge carrier density and high mobility of a charge in semiconductor makes them very important in this aspect. The energy band gap of semiconductor ranges from 0.3 to 3.5eV. The practical magnitudes of the dimensions of the samples are in micrometers to be compatible with the magnitudes of the parameters of the illuminating radiations. The thermal equilibrium charge carrier concentration ranges from $10^{12}cm^{-3}$ in the intrinsic semiconductor to $10^{19}cm^{-3}$ in the highly doped non-degenerate semiconductor. The mobility of free carriers in semiconductor also ranges from $10^{2}cm^{2}V^{-1}s^{-1}$to $10^{4}cm^{2}V^{-1}s^{-1}$.

The practical density of room temperature thermal equilibrium majority carrier for semiconductor that was determined using Hall Effect measurement is ranged from $10^{12}cm^{-3}$ for intrinsic semiconductor to $10^{19}cm^{-3}$ for highly doped non-degenerate semiconductor, and the density of minority carrier concentration is also ranged from $10^{12}cm^{-3}$ for intrinsic semiconductor to $10^{5}cm^{-3}$ for highly doped non-degenerate semiconductor. The room temperature mobility of electrons for most semiconductors is ranged from $10^{3}cm^{2}V^{-1}s^{-1}$ to $10^{4}cm^{2}V^{-1}s^{-1}$ and that of holes is also ranged from $10^{2}cm^{2}V^{-1}s^{-1}$to $10^{3}cm^{2}V^{-1}s^{-1}$[7].

The energy band gap of small direct band gap semiconductor is ranged from 0.3eV to 1.1eV [8].

The room temperature carrier capture coefficients by different energy states representing these recombination mechanisms in different semiconductors were determined by different researchers to be ranged from $10^{-29}cm^{6}s^{-1}$ for Auger recombination mechanism to $10^{-10}cm^{3}s^{-1}$ for Radiative recombination mechanism [1].

Small band semiconductors with energy band gap ranged from 0.3 to1.0eV, like indium arsenide (InAs), gallium antimonide (GaSb) and etc., are characterized by the absence or small amount of impurity materials, presence of very high charge carrier concentration and high charge carrier mobility. This makes this semiconductor a promising material for the fabrication of high frequency optoelectronic devices working in the wide range of infrared region [8]. In recent years, considerable progress has been made in the fabrication of

optoelectronic devices working at different frequency ranges in the infrared region using small band gap materials. Small band gap materials are used in various domains, such as pollutant detection and infrared thermal imaging, using a variety of device architectures, including near infrared photo-detectors, resonant tunneling structures and other quantum devices [9, 12]. Some of these semiconductors are also used as booster cells in solar cell clusters to improve the efficiency of photovoltaic and thermo-photovoltaic (TPV) cells [4, 11, and 13].

Semiconducting materials have been of scientific interest for almost 200 years. The discovery of semiconductors is generally attributed to Michael Faraday, who in 1833 published a description of a material with a resistivity which had the opposite temperature dependence to that typically measured for metals [6]. Forty years later in 1873, Warren Smith observed that the resistivity of a semiconductor reduced when it was illuminated. The use of semiconductors in devices followed the discovery of a preferential direction for current flow through metal contacts made to naturally occurring crystals by Carl Braun in 1874 [58].

The importance of the semiconductor materials lies in their flexibility of controlling their properties [58]. For most of the device applications, semiconductor is doped with impurities. In the case of silicon, an IV-group element, III or V-group elements are used as impurities. These impurities control the type and conductivity properties of silicon. III-group impurities act like acceptors and the V-group impurities act like donors in silicon. The ionization energies of these impurities are low, and hence the energy level of these impurities are close to the band edge. Therefore, these impurities are generally referred to as shallow level impurities. These shallow level impurities are widely used in the fabrication of semiconductor devices like p-n junctions, Zener diodes, tunnel diodes, transistors, power devices, junction lasers etc. The fundamental properties such as ionization energies and capture cross-sections of these shallow levels are adequately understood in terms of the hydrogenic model in the effective mass approximation [59,60], and the others are deep levels. The presence of deep levels affects the electrical and optical characteristics of the solid state devices. Sometimes, these deep levels may be helpful or sometimes detrimental. For example, impurities like gold and platinum are used as lifetime killers as these impurities provide additional recombination paths to the carriers and hence reduce the minority

carrier lifetime. Radiative recombination centers are useful in giving different colours in light emitting diodes and phosphors. Chalcogene (S, Se and Te) are used in silicon infrared (IR) detectors. Deep levels are source of low frequency noise in semiconductors. Since deep levels generally act as non-radiative recombination centers, the quantum efficiency light emitting diodes or the junction lasers is reduced and also the transfer efficiency reduce [61]. Deep levels may be intentional or unintentional. Therefore, it is necessary to characterize them to have better control over the device performance. Complete characterization of deep levels needs to find their charge states, energy level, degeneracy ratio, concentration, capture cross-section and chemical identity. It is also desirable to know the defect structure of the complexes and the symmetry of the deep impurity in the host lattice [62].

Semiconductors have electrical conductivities between metals and insulators. The conductivity of these materials can be varied over orders of magnitude by changes in temperature, optical excitation, and impurity content without altering the band-gap and other basic parameter of the host material [58] and by simply doping it with acceptor or donor impurities or by using external excitations. At low temperatures, a pure semiconductor may become a perfect electrical insulator, since its valence band is totally filled with valence electrons and the conduction band is completely empty. However, as the temperature rises, a fraction of the valence electrons is excited into the conduction band by the thermal energy, thus creating free holes in the valence band. As a result, the electrical conductivity will increase rapidly with increasing temperature. Therefore, even an intrinsic semiconductor may become a good electrical conductor at high temperatures. In general, the semiconductors may be divided into two categories: the pure un-doped semiconductor, which is usually referred to as the intrinsic semiconductor, and the doped semiconductor, which is also called the extrinsic semiconductor. Another distinct difference between a metal and a semiconductor is that the electrical conduction in a metal is due to electrons, while the electrical conduction of a semiconductor may be attributed to electrons, holes, or both carriers. The electrical conduction of an intrinsic semiconductor is due to both electrons and holes, while for an extrinsic semiconductor it is usually dominated by either electrons or holes, depending on whether the semiconductor is doped with shallow donors or shallow acceptor impurities. To understand the conduction mechanisms in a semiconductor, the equilibrium properties of a semiconductor are first examined. A unique feature of

semiconductor materials is that the physical and transport parameters depend strongly on temperature. For example, the intrinsic carrier concentration of a semiconductor depends exponentially on temperature. Other physical parameters, such as carrier mobility, resistivity, and the Fermi level in a non-degenerate semiconductor, are likewise a strong function of temperature. In addition, both the shallow-level and deep-level impurities may also play an important role in controlling the physical and electrical properties of a semiconductor. For example, the equilibrium carrier concentration of a semiconductor is controlled by the shallow-level impurities, and the minority carrier lifetimes are usually closely related to defects and deep-level impurities in a semiconductor. The general expressions for the electron density in the conduction band and the hole density in the valence band are derived for the cases of the single spherical energy band and the multi-valley conduction bands.

The column IV semiconductors, silicon and germanium are called elemental semiconductors because they are composed of single species of atoms. Compounds of column III and V atoms, as well as certain combinations from II and VI, and from IV, make up the compound semiconductors. Every solid has its own characteristic energy band structure. This variation in band structure is responsible for the wide range of electrical characteristics observed in various materials. In metals, the bands either overlap or are only partially filled. Thus, in metals, high electrical conductivity is due to the fact that electrons and empty energy states are intermixed within bands so that electrons can move freely under the influence of an electric field. Consider a valence band in ground state. The total crystal Momentum for this band is zero, as for every occupied k state; there exists a corresponding filled state with opposite momentum. The top of valence band for most semiconductors occurs at zero k. The bottom of the conduction band in direct semiconductors occurs at zero k . Such semiconductors respond to external light, as the valence and conduction band edges are aligned in direct semiconductors.

The purpose of this work is in particular to determine the effect of Auger recombination on the photocurrent produced in a direct band gap semiconductor during illumination with a light of photon energy is greater than the energy band gap semiconductor.

The valence band maximum in most semiconductors is at the T point and has three branches: the heavy hole band with the smallest curvature, a light hole band with a larger curvature,

and a split-off band at a different energy. If the conduction band electron and the hole are created by the excitation of a valence band electron to the conduction band, they are called an electron-hole pair (EHP). After excitation to the conduction band, an electron is surrounded by a large number of unoccupied energy states [27].

The radiative generation-recombination and Auger mechanisms are fundamental band-to-band processes which are determined by the electronic band structure of the semiconductor. The role of radiative mechanism in detection of IR radiation has been recently critically reexamined by Humpreys. The Auger mechanism dominates generation and recombination processes in high quality and small band gap semiconductor. The band-to-band Auger effects are classified in several processes according to related bands. Auger recombination mechanisms are possible in a semiconductor with a single conduction band and heavy, light-hole and Split off valence bands [21]. Radiative recombination is relatively unimportant in indirect band-gap semiconductors, because the radiative lifetime is extremely high. Auger recombination is typically observed in both direct and indirect band-gap semiconductors when either the doping density or the excess carrier density is very high. Similar to the radiative lifetime, the Auger lifetime is independent of any impurity density. Auger recombination is the ultimate recombination mechanism for devices operating at very high injection or at very high doping densities. It is also the dominant recombination mechanism for narrow band-gap semiconductors. Both radiative and Auger recombination can also occur through intermediate energy levels. When electron-hole pairs recombine radiatively through intermediate levels, photons are generally emitted for only one of the transitions. This recombination mechanism is used in light-emitting phosphors that are deliberately doped with impurities of a particular kind to generate light of a particular wavelength [66].

Gallium antimonide (GaSb) and related compounds are direct band-gap semiconductors suitable for fabricating high-frequency electronic devices and optoelectronic devices. The photo response of this material makes it very useful in the design of a variety of device architectures, including photo detectors, resonant tunneling structures and other quantum devices. The performance of the material in this case depends on the lifetime of free charge carriers generated by the interaction of light with the material, referred to as the excess carrier lifetime (τ) [11]. Using the results from Hall Effect measurements along with the

relations describing the lifetimes of the excess minority carriers in the bulk of the semiconductors, the theoretical values of the effective excess carrier lifetime in the materials were also calculated [9,11].

Therefore, radiative lifetime is constant at low injection, but then decreases and continues to decrease as the injection level increases. While radiative recombination is typically the dominant recombination process in direct bandgap semiconductors under low injection level, it is considered to be small or even negligible compared to other recombination processes in indirect semiconductors. Radiation which is presumably due to the recombination of free electrons and holes has been observed in gallium antimonide (GaSb). The radiative lifetime is inversely proportional to the total concentration of free carriers under all circumstances [50]. Auger recombination will become the dominant mode of recombination in indirect semiconductors for high injection levels. The lifetimes increased then decreased with increasing excess carrier density. This is due to effects of Auger recombination and Radiative recombination and the lifetimes were taken at a consistent excess carrier concentration [52]. The lifetime of both radiative and Auger mechanisms decreases with increase in doping concentration and the effective lifetime of the carriers is controlled only by Auger mechanism [64]. Schmidt (1999) measured carrier recombination lifetime on the intrinsic semiconductor, he recorded the lifetime values higher than 1.1ms at an injection level of $1\times10^{16}\text{cm}^{-3}$ which fell to 0.1ms at $1\times10^{17}\text{cm}^{-3}$ by Auger recombination as indicated by the inverse quadratic dependence of the lifetime on excess carrier concentration [27].

The general objective of this work is to study the Effects of impact ionization on the Photo response of a direct small band-gap bulk semiconductor as compared to the optical generation effect. The specific objectives are to describe:

- the doping effect on the impact ionization and optical generation,
- the temperature effect on the impact ionization and optical generation and
- the injection of free carriers on the impact ionization and optical generation in small and direct band gap semiconductors like GaSb.

The thesis organized in five chapters. Chapter 2 deals with the theory of energy band-gap semiconductor, thermal equilibrium properties of semiconductors and photo-response of semiconductors. Equations governing the recombination lifetimes for the two basic

recombination mechanisms depicted are derived in this Sections. That is, Auger and Radiative recombination mechanisms in a semiconductor are also discussed. Chapter 3 presents the characterization techniques that have been used in this work and methods of determining the lifetimes in a semiconductor. Chapter 4 describes the results obtained at the end of the different methods performed. In this section, the concepts of Impact ionization and the effects it has on the photo-response of the materials will be described in detail. Chapter 5 concludes the entire parts of this work and describes the results obtained in chapter 4.

Chapter 2

Literature Review

2.1. Thermal Equilibrium Properties of Semiconductors

In the section, the general properties of an isolated semiconductor under different conditions. These properties may include the energies of the charge carriers and the free charge carrier concentrations at various temperature.

2.1.1 Energy Band-gap

In a solid, the energy difference between the top of valance band (E_V) and the bottom of conduction band (E_C) is defined as the band-gap energy (E_g). The band-gap energy of a semiconductor defines its optical absorption threshold for the photoelectric effect. That is, generation of electric charge-carrier from light absorption only occurs with photons with energies greater or equal to the band gap, E_g (or $h\upsilon \geq E_g$), where E_g is the energy band gap of the given semiconductor, h the Planck's constant and υ, the frequency of the absorbed photon by the semiconductor. When supra-band-gap light is absorbed by a semiconductor, charges move between the valence and conduction bands [39]. When a semiconductor is illuminated by a photon of energy greater than its energy band gap ($h\upsilon > E_g$), electron-hole pairs are generated in the semiconductor. The photo-response of the semiconductor can be described through the current produced due to the electron-hole pairs produced in the process. Hence, the amount of current produced by these charge carriers is also affected by the effective lifetime of the carriers.

The band gap energy $E_g = E_C - E_V$, is perhaps the most important in semiconductor physics. A contraction of the crystal lattice with decreasing temperature usually leads to a strengthening of the interatomic bonds and an associated increase in the band gap energy. The first empirical relation for the band gap shift with temperature was developed by Varshni et al [24]. The temperature dependence of the energy band-gap, $E_g(T)$ has been experimentally determined yielding the following expression as a function of the temperature, T:

$$E_g(T) = E_g(0) - \frac{\alpha T^2}{T + \beta}, \quad (1)$$

where α and β are constants chosen to obtain the best fit to experimental data and $E_g(0)$ is the limiting value of the band at zero Kelvin.

2.1.2 Thermal Equilibrium Carrier Concentration

The density of free electron carriers, n_0 in the conduction band for the non-degenerate semiconductor case can be simplified to:

$$n_0 = N_C \exp\left(-\frac{E_C - E_F}{k_B T}\right), \quad (2)$$

where

$$N_C = 2\left(\frac{2\pi m_n^* k_B T}{h^2}\right)^{3/2} \quad (3)$$

is the density of state in the conduction band and m_n^* is effective mass of electrons in the conduction band. The density of the hole carriers, n_0 in the valence band can be derived also for non-degenerate case as:

$$p_0 = N_V \exp\left(-\frac{E_F - E_V}{k_B T}\right), \quad (4)$$

where

$$N_V = 2\left(\frac{2\pi m_p^* k_B T}{h^2}\right)^{3/2} \quad (5)$$

is the density of state in the valence band and m_p^* is the effective mass of holes in the valence band.

2.1.3 Intrinsic Semiconductors

Un-doped semiconductors (i.e., semiconductors with no intentional doping) [49] or a perfect semiconductor crystal with no impurities or lattice defects is called an *intrinsic semiconductor*. A semiconductor may be considered as an intrinsic semiconductor if its thermally generated carrier density represented by n_i is much larger than the background doping or residual impurity densities. At T = 0 K, an intrinsic semiconductor behaves like an insulator because the conduction band states are totally empty and the valence band states are completely filled. However, as the temperature increases, some of the electrons in the valence band states are excited into the conduction band states by thermal energy, leaving

behind an equal number of holes in the valence band and the electron-hole pairs are produced. These electron-hole pairs (EHPs) are the only charge carriers in intrinsic material [20]. Therefore, the intrinsic carrier density increases with increasing temperature. Suppose that $\mathfrak{N}$ is the concentration of electron-hole pairs thermally generated in the respective bands and n_R is the concentration of electron-hole pairs annihilated after the generation, the free carrier concentrations in the conduction and valence bands adjust for the intrinsic semiconductor to:

$$n_0 \approx \mathfrak{N} - n_R = n_i = p_0. \tag{6}$$

As we discussed in the above section, the electron-hole pairs in an intrinsic semiconductor are generated by thermal excitation. Therefore, for intrinsic semiconductors with an energy band gap on the order of 1eV or higher, the intrinsic carrier density is usually very small at low temperatures below 100K. As a result, the resistivity for these intrinsic semiconductors is expected to be very high at low temperatures.

Since the non-degenerate relations are obviously valid for an intrinsic semiconductor where the Fermi level, E_F is equal to the intrinsic level energy, E_i the semiconductor,

$$n_i = N_V \exp\left(-\frac{E_i - E_V}{k_B T}\right) = N_C \exp\left(-\frac{E_C - E_i}{k_B T}\right). \tag{7}$$

The intrisic energy, E_i can be written from Eqn. (7) as:

$$E_i = \left(\frac{E_V + E_C}{2}\right) + \frac{3}{4} k_B T \ln\left(\frac{m_p^*}{m_n^*}\right). \tag{8}$$

If E_V and E_C are known at a certain temperature, one can easily compute the values of n_i as function of temperature. The intrinsic concentration, n_i for free carriers the corresponding bands can be computed from equations (2) and (4) above as:

$$n_i = \sqrt{p_0 n_0} = \sqrt{N_V N_C} \exp\left(\frac{E_g}{k_B T}\right). \tag{9}$$

Equation (9) is called the *law of mass action*.

2.1.4 Extrinsic Semiconductors

In addition to the intrinsic carriers generated thermally, it is possible to create carriers in semiconductors by purposely introducing impurities into the crystal. This process, called *doping*, is the most common technique for varying the conductivity of semiconductors. By doping, a crystal can be altered so that it has a predominance of either electrons or holes.

Thus there are two types of doped semiconductors, n-type (mostly electrons) and p -type (mostly holes). When a crystal is doped such that the equilibrium carrier concentration n_0 is different from the intrinsic carrier concentration n_i the material is said to be extrinsic. When impurities or lattice defects are introduced into an otherwise perfect crystal, additional levels are created in the energy band structure, usually within the band gap. This level is filled with electrons at 0 K, and very little thermal energy is required to excite these electrons to the conduction band. As the temperature is raised, these electrons are donated to the conduction band, and at about 100K all the donor atoms are ionized. This temperature range from 0 K to 100 K is called the *partially ionization region*. Once, the donors are ionized, the conduction band electron concentration is $n_0 \sim N_d = 10^{16}\text{cm}^{-3}$, N_d donor impurity atoms, since one electron is obtained for each donor atom. When every available extrinsic electron has been transferred to the conduction band, n_0 is virtually constant with temperature until the concentration of intrinsic carriers n_i becomes comparable to the extrinsic concentration N_d . Finally, at higher temperatures n_i is much greater than N_d , and the intrinsic carriers dominate. In most devices it is desirable to control the carrier concentration by doping rather than by thermal EHP generation. Thus, one usually dopes the material such that the extrinsic range extends beyond the highest temperature at which the device is to be used [57].

The most important and unique feature of a semiconductor material lies in the fact that its electrical conductivity can be readily changed by many orders of magnitude by simply doping the semiconductor with shallow-donor or shallow-acceptor impurities. By incorporating the doping impurities into a semiconductor, the electron or hole density will increase with increasing shallow-donor or shallow-acceptor impurity concentrations. For example, electron or hole densities can increase from 10^{13}cm^{-3} to more than 10^{20}cm^{-3} if a shallow-donor or shallow-acceptor impurity with an equal amount of impurity densities were added into a silicon crystal. In addition to the relatively shallow-level donors and acceptors, the substitution of other impurity atoms into a host semiconductor can give rise to deep-level states allowed states in the band gap more than a few tenths of an eV from either band edge. These are commonly referred to as traps or recombination-generation centers. Such centers are usually unintentional impurities, are not necessarily ionized at room temperature, and typically occur in concentrations far below the dopant concentration.

The deep level centers can be donor-like (positively charged when empty and neutral when filled with an electron), acceptor-like (neutral when empty and negatively charged when filled with an electron), or may exhibit multiple charge states with associated multiple levels in forbidden gap.

As discussed above, adding donor or acceptor impurity atoms into semiconductor will change the distribution of electrons and holes in the material, and as a result, the position of Fermi energy will change. Eliminating N_C and N_V among Eqns. (2), (4) and (5) yields:

$$n_0 = n_i \exp\left(-\frac{E_i - E_F}{k_B T}\right) \quad \text{and} \quad p_0 = N_C \exp\left(-\frac{E_F - E_i}{k_B T}\right). \tag{10}$$

The law of mass action, Eqn. (9) allows one to calculate the minority carrier density in an extrinsic semiconductor when the majority carrier density is known [2].

$$\text{Minority carrier density} = \begin{cases} \frac{n_i^2}{p_0}, & \text{for p} - \text{type material,} \\ \frac{n_i^2}{n_0}, & \text{for n} - \text{type material.} \end{cases} \tag{11}$$

The thermal equilibrium extrinsic Fermi-level, E_F can also be described from Eqn. (10) in terms of E_i and the thermal equilibrium carrier concentrations as:

$$E_F = E_i - k_B T \ln\left(\frac{p_0}{n_i}\right) = E_i + k_B T \ln\left(\frac{n_0}{n_i}\right). \tag{12}$$

As the charge carrier concentrations change, the position of the extrinsic Fermi energy level varies within the band gap until the system reaches thermal equilibrium. Equation (12) shows that E_F lies above E_i for n-type material ($n_i > p_o$) and below E_i for p – type material ($n_i < p_o$) [2].

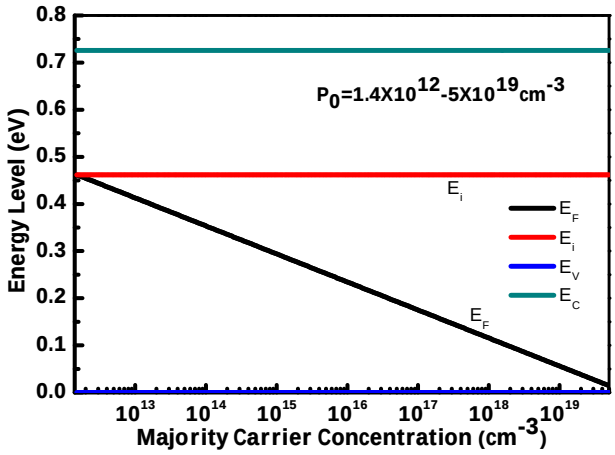

Figure 2-1: Variation of Fermi Energy with Doping Concentration.

Figure 2.1 shows the Fermi energy level as a function of donor concentration (n-type) and as a function of acceptor concentration (p-type). As the doping level increases the Fermi energy level moves closer to the valence band for the p-type material and closer to conduction band for the n-type material. Now, as doping concentration increases the Fermi energy level moves closer to the valence band because the material is p-type.

If the Fermi energy level lies inside the conduction (or valence) band, the material is referred to as a degenerate semiconductor. The semiconductor becomes degenerate at high carrier concentrations above $p_0 = 10^{19}\text{cm}^{-3}$ [56]. In this case, the exponential approximation to the Fermi function cannot be used, so that the carrier concentrations must then be obtained by numerical solution. Under conditions of very heavy doping, the donor (acceptor) impurity band actually merges with the conduction (valence) band to become what is called the band tail. This results in an effective decrease of the band-gap.

At high temperature the semiconductor material begins to lose its extrinsic characteristics and begins to behave more like an intrinsic semiconductor. Figure 2.2 illustrates the temperature variation of semiconductor energies.

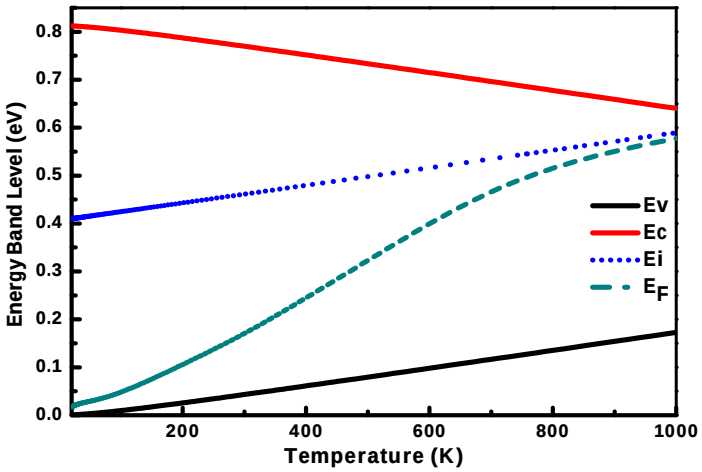

Figure 2-2: illustrates the temperature variation of semiconductor energies.

As one can see from Figure 2-2, both E_C and E_V become closer and closer to the mid-gap with increasing temperature, as a result the band gap energy decreases with increasing temperature. One can easily see from Eqn. (8) that, if the electron and hole effective masses are equal, $m_p^* = m_n^*$ the intrinsic Fermi level, E_i is exactly in the center of the band gap. The intrinsic Fermi level, E_i moves toward the conduction band edge for $m_p^* > m_n^*$ for p-type material and toward the valence band edge if $m_p^* < m_n^*$ for n-type material.

2.1.5. Charge neutrality

When free electron-hole pairs annihilate through recombination, the free carrier concentrations in the conduction and valence bands adjust for the intrinsic semiconductor to Eqn. (12). For the extrinsic semiconductors this takes the form:

$$n_0 = N_d^+ + \mathfrak{R} - n_R \qquad \text{and} \qquad p_0 = N_a^- + \mathfrak{R} - n_R, \tag{13}$$

where n_R is the concentration of the total electron-hole pairs being annihilated each other after the donors and the acceptors are being ionized, $\mathfrak{R}$ is the concentration of electron-hole pairs thermally generated from band to band, N_d^+ and N_a^- are the densities of free electrons and holes contributed by the donor and the acceptor levels to the respective conduction and valence bands. Upon eliminating $\mathfrak{R} - n_R$ in Eqn. (13), the well-known neutrality relationship is obtained:

$$n_0 + N_a^- = p_0 + N_d^+ \tag{14}$$

The density of the ionized impurities at both the donor and acceptors are given by:

$$N_d^+ = \frac{N_d}{1 + 2\exp\left(\frac{E_F - E_d}{k_B T}\right)} \qquad \text{and} \qquad N_a^- = \frac{N_a}{1 + 4\exp\left(\frac{E_a - E_F}{k_B T}\right)}. \tag{15}$$

The law of mass action (Eqn. (9)) along with Eqn. (15) yields:

$$p_0 = \frac{N_a^- - N_d^+}{2}\sqrt{n_i^2 + \left(\frac{N_a^- - N_d^+}{2}\right)^2}, \qquad n_0 = \frac{N_d^+ - N_a^-}{2}\sqrt{n_i^2 + \left(\frac{N_d^+ - N_a^-}{2}\right)^2} \tag{16}$$

For very high acceptor impurity concentration $N_a^- \gg N_d^+$ and $N_a^- > n_i$, Equation (16) can be simplified:

$$\frac{p_0}{n_i} \approx \frac{N_a^-}{n_i} + \frac{n_i}{N_a^-} > 1, \quad \Rightarrow p_0 > n_i, \qquad \frac{n_0}{n_i} \approx \frac{n_i}{N_a^-} < 1, \qquad \Rightarrow n_0 < n_i \tag{17}$$

It can be seen from Eqn. (17) that the addition of different acceptor and donor impurity concentrations to the semiconductor increases the majority carrier concentration above the intrinsic level and decreases the minority carrier concentration below the intrinsic level. If the acceptor and the donor impurity concentrations are equal (i.e. completely compensated material), Eqn. (16) becomes:

$$p_0 = n_0 \approx n_i. \tag{18}$$

Hence, having equal concentrations of conduction band electrons and valence band holes is a property of intrinsic semiconductors. Thermal equilibrium conditions do not allow this for a system with different donors and acceptor concentrations. A carrier generated from an impurity level can stay free provided its concentration exceeds that of oppositely charged carriers generated from another impurity in the material. If the acceptor and donor impurity concentrations are equal, the material again behaves like an intrinsic semiconductor. Using Eqn. (15) and (14) for sufficiently low temperatures yields:

$$n_0 + \frac{N_a}{1 + 4\exp\left(\frac{E_a - E_F}{k_B T}\right)} = p_0 + \frac{N_d}{1 + 2\exp\left(\frac{E_F - E_d}{k_B T}\right)}. \quad (19)$$

For p-type material, the Fermi level lies below mid-gap (closer to the valence band) as discussed earlier $E_F \ll E_d$. The exponential factor in the denominator of the last term on the right hand side of Eqn. (19) can thus be neglected for low and high temperature values. This means that almost all the donor impurities are ionized, regardless of the temperature. With this assumption, Eqn. (19) becomes:

$$n_0 + \frac{N_a}{1 + 4\exp\left(\frac{E_a - E_F}{k_B T}\right)} = p_0 + N_d. \quad (20)$$

At sufficiently low temperatures, $p_0, n_0,$ and N_a^- all vary with temperature, and as a result the intrinsic concentration n_i also increases with temperature. This region in which N_a^- varies with temperature is called the partial ionization region. When the temperature is increased beyond the partial ionization region, the acceptor level is completely ionized and Equ. (20) becomes.

$$n_0 + N_a = p_0 + N_d. \quad (21)$$

The temperature ranges in which the acceptor level is completely ionized and $p_0 \approx N_a$ is known as the *complete ionization* region. As we can see from Eqn. (21), the difference between n_0 and p_0 is constant, i.e. the concentrations of holes and electrons increase by the same amount due to the increment in intrinsic concentration. Since the change in intrinsic concentration does not affect the majority carrier concentration, p_0 remains constant and is equal to N_a.

The concentrations of holes and electrons increase by the same amount due to the increment in intrinsic concentration. Upon a further increase in temperature (beyond the

extrinsic region), the intrinsic concentration n_i begins to dominate. Both the majority and minority carrier concentrations approach the intrinsic concentration and the semiconductor enters a quasi-intrinsic region.

Figure 2-3 shows (a) four regions in which a simulation of variations in majority carrier concentration varies as a function of temperature for the p-type semiconductor of acceptor density 10^{16} cm^{-3} being analyzed, (b) the simulation extended to other samples of the same materials with different acceptor concentrations. Region I is a range in which N_a^- varies with temperature (partial ionization region). Region II in Figure 2-3 (a) is the temperature range of extrinsic region in which the acceptor level is completely ionized (complete ionization region). Region III is the transition region between the completely ionization and intrinsic regions. The boundaries of this region are not clearly defined [2]. Region IV is the region in which both the majority and minority carrier concentrations become equal and approach the intrinsic concentration (quasi-intrinsic region).

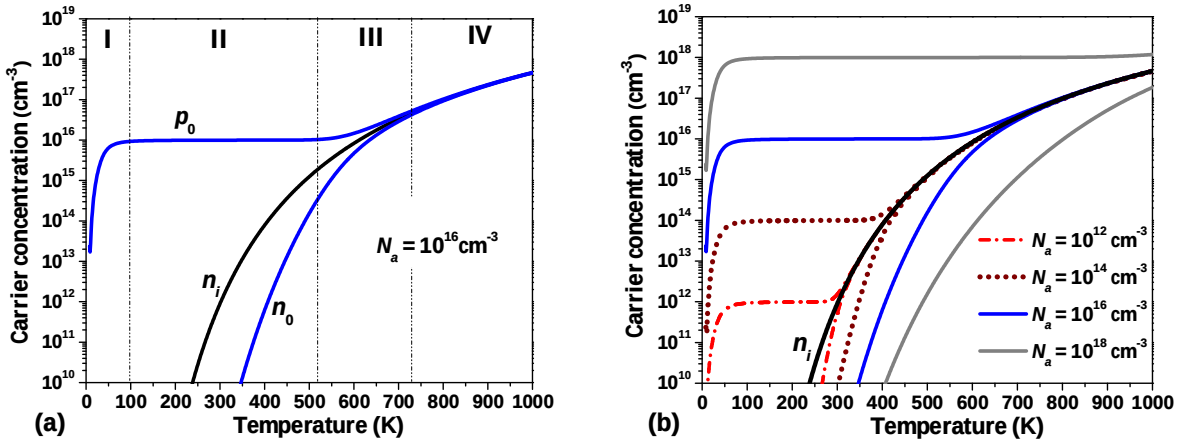

Figure 2-3: (a) four regions in which a simulation of variations in majority carrier concentration varies as a function of temperature for p-type semiconductor of acceptor density 10^{16} cm^{-3} being analyzed, (b) the simulation extended to other samples of the same materials with different acceptor concentrations.

Figure 2-3 (b) shows that, the range of the complete ionization region (Region II) increases towards the higher temperature region with increasing the doping level, so that, the lower edge of the intrinsic region shifts to the higher temperature region with the increase in the acceptor or donor concentrations. There is no significant change in the partial ionization region (region II) with increasing the shallow acceptor or donor level. However, the partial ionization region shifts to the higher temperature region for deep acceptor or donor level.

2.1.6 Hall Effect

Hall Effect measurements is a useful technique for characterizing the electrical transport properties of metals and semiconductors. Edwin Hall discovered this effect in 1879. A Hall Effect measurement system can actually be used to determine quite a few material parameters, but the primary one is the Hall voltage (V_H) and it is a system used to measure a material's electrical properties such as: carrier mobility, carrier concentration (n), Hall coefficient (R_H), resistivity (ρ), and the conductivity (σ) type (N or P) are all derived from the Hall voltage measurement [15]. The Hall Effect measurement gives a direct measure of free carrier type and density which, when combined with a resistivity measurement on the same sample, also yields a value for the appropriate carrier mobility. Hall measurement is the most widely used to test electrical quality of semiconductor materials. The motion of free carriers in a solid under the combined influence of magnetic and electric fields has been studied for over a century [20].

2.2 Photo-response of semiconductors

The interaction of light with matter can be viewed macroscopically as consisting of four components: incident, reflected, transmitted and absorbed (or scattered) components. The photo-response of the material can be measured through the change in the photoconductivity due to the photo-generated free carriers or. In this section, the effects the recombination of free carriers causes on the performance of semiconductor materials is described in detail.

2.2.1 Band to Band Recombination Mechanisms in Semiconductors

Optically generated charge carriers can recombine in two different ways: radiatively or non-radiatively. Radiative recombination is the opposite of optical generation of charge carriers. It occurs when the energy of the excited electron is emitted by the formation of a photon during the annihilation of an EHP. Non-radiative recombination occurs when excess energy is released as phonons or transferred as excess kinetic energy to another charge carrier, *i.e.* the excess energy is dissipated as heat during the recombination process.
Several mechanisms may be considered for the recombination of free carriers in semiconductors. Auger recombination mechanism which the reverse of Impact of ionization

in solid materials was first considered by Skinner (1940) [33]. In connection with non-metals it was first discussed by Frohlich & O'Dwyer (1950) [33, 27]. The other two which have received most attention so far are Radiative recombination (Roosbroeck &Shockley 1954) and recombination via traps or Shockley-Read-Hall (SHR) recombination (1952) [33]. In their present forms, these are not entirely successful in explaining the experimental lifetimes of excess carriers. The former mechanism gives in many cases values which are too large, as in the case of germanium, silicon and indium antimonide (InSb). With the model of recombination via traps it is often possible to explain the shapes of lifetime curves as a function of temperature or carrier concentration. This explanation of shape depends on a suitable choice of two adjustable parameters, which represent the mean capture rate of electrons and holes by traps. Since no well-tested theory exists for these parameters, one cannot be certain that, even when an explanation of the shape of a curve has been given, the mechanism itself is fully understood (Breckenridge 1956). One of the processes which have not yet been fully investigated is recombination by the Auger effect. Although it has repeatedly been mentioned in connection with lifetime problems in semiconductors, two relevant calculations (Pincherle 1955; Bess 1957) have been published. These are in the nature of estimates only, owing to the author's desire to circumvent the rather delicate problems posed by the integration of the transition probability over all states. The Auger effect may be thought of as a two-electron or a two-hole collision, the energy lost by one electron being taken up by another. This study reveals the effects brought by the Auger recombination (or impact ionization) to the performance of a small direct band gap semiconductor [27].

Recombination of electrons and holes is a process by which both carriers (electrons and holes) annihilate each other through one or multiple steps. Both carriers eventually disappear from electric conduction in the process. The energy difference between the initial and final state of the electron is released in the process. This leads to one possible classification of the recombination processes. In the case of Radiative recombination, this energy is emitted in the form of a photon. In the case of non-Radiative recombination, it is passed on to one or more phonons, as in the case of SRH recombination mechanism and in the case of Auger recombination it is given off in the form of kinetic energy to another

electron. Another classification scheme considers the individual energy levels and particles involved.

In Auger recombination process, three carriers participate, either two electrons and one hole, or two holes and one electron. The momentum of the two recombining carriers and the energy liberated during recombination are imparted to the third surviving carrier as kinetic energy. Direct band-to-band Radiative recombination process occurs in direct band gap semiconductors like GaAs, GaAsP, InP etc., which are therefore used for the fabrication of optoelectronic devices. But it is unlikely in indirect band gap semiconductors such as Si and Ge. The rate of recombination is proportional to the concentrations of electrons as well as holes.

A) Radiative recombination mechanism

Radiative recombination is a direct recombination mechanism, in which the electrons in the conduction band decay to the valence band (*i.e.* recombine with holes in the valence band). This is a very efficient process in direct band gap semiconductors. The energy lost by an electron in making the transition is released as a photon. The total recombination rate (U_R) is directly proportional to the product of the concentration of electrons n available in the conduction band and the concentration of holes p available in the valence band:

$$U_R = C_R np, \tag{22}$$

where C_R is a constant known as the coefficient of holes in the valence band for the capture of electrons, and is related to the electron capture cross-section (σ_R) and the thermal velocity of the electrons (ϑ_{th}) [2, 22, and 23]:

$$C_R = \sigma_R \vartheta_{th}. \tag{23}$$

The band-to-band capture coefficient for bands with spherical symmetry was shown by van Roosbroeck and Shockley to depend on the absorption coefficient through the relation:

$$C_R = \frac{8\pi k_\infty}{c^2} \int_0^\infty \frac{\alpha(\upsilon)\upsilon^2 d\upsilon}{\exp\left(\frac{h\upsilon}{k_B T}\right) - 1}, \tag{24}$$

where $\alpha(\upsilon)$ the absorption coefficient, h is Planck's constant and c is the speed of light. Values of C_R can be obtained by numerical integration of Eqn. (24) for narrow band gap semiconductors as [2, 22, and 26]:

$$C_R = e\pi\sqrt{k_\infty}\left(\frac{m_n}{m_n^* + m_p^*}\frac{300}{T}\right)^{\frac{3}{2}}\left(1 + \frac{m_n}{m_n^*} + \frac{m_n}{m_p^*}\right)\left[E_g^2 + 3E_g k_B T + 3.75 k_B^2 T^2\right], \quad (25)$$

where E_g and $k_B T$ are in electron volt (eV).

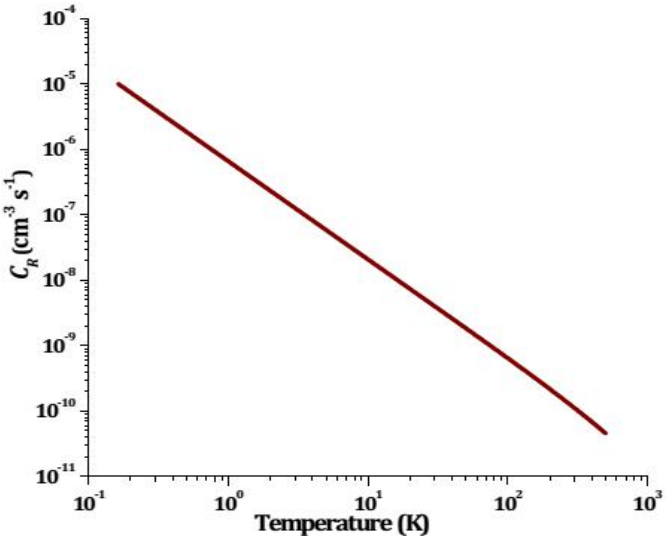

Figure 2-4: Radiative recombination coefficient as function of temperature for GaSb.

For large band gap materials where $E_g \gg k_B T$ only the E_g^2 term is needed. Figure 2.4 shows the radiative recombination coefficient as function of temperature. As we observed from the figure the radiative coefficient decreases with temperature increases and increases as the temperature decreases. Since, $E_g \gg k_B T$ the term E_g^2 is dominant in this case as predicted. The net photo-generated carrier recombination rate in the absence of excess carrier traps is given by the difference between the non-thermal equilibrium recombination rates.

But, in non-equilibrium electron-hole densities, $np > n_i^2$ and $\delta n = n - n_{o,}\ \delta p = p - p_o$. In a non-degenerate semiconductor, the rate at which electrons and holes are annihilated via band-to-band Radiative recombination is proportional to the product of electron and hole densities in the conduction and valence bands.

The Radiative recombination rate (U_{Rad}), depends on the concentration of free electrons (n) and holes (p) is obtained as follows [23]:

$$U_R = C_R\left(np - n_i^2\right). \quad (26)$$

Inserting non-equilibrium concentration $n = n_o + \delta n$ and $p = \delta p + p_o$ into equation (26) and for the case of low-level injection, the excess carrier concentration δn and δp with $\delta n = \delta p$, then the following general expression for radiative recombination rate, U_R is given by:

$$U_R = C_R \delta n(\delta n + p_o + n_o) \tag{27}$$

So, the radiative excess carrier lifetime, τ_R takes the form:

$$\tau_R = \frac{\delta n}{U_R} = = \frac{1}{C_R(n_o + p_o + \delta n)} = \frac{\tau_{R0}}{1 + C_R \tau_{R0} \delta n}, \tag{28}$$

where

$$\tau_{R0} = \frac{1}{C_R(n_o + p_o)}.$$

For a material under low injection level ($\delta n \ll p_0 + n_0$), so that:

$$\tau_R = \tau_{R0}. \tag{29}$$

For a material under high injection level ($\delta n \gg p_0 + n_0$), then:

$$\tau_R = \frac{1}{C_R \delta n}. \tag{30}$$

B) Auger recombination mechanism

There are two types of Auger recombination coefficients depending on their carrier type.

i. *Electron Auger capture coefficient*

The dominant Auger process in n-type material is band-to-band Auger recombination, called the Auger 1 (CHCC) process, in which a conduction band electron recombines with a heavy hole (C-H) and a conduction electron is excited to a higher energy level (C-C). This mechanism is developed by Beattie and Landsberg for InSb like band structures. The Auger 1 electron capture coefficient is given by [2, 26]:

$$C_{na} = \frac{8e^4(2\pi)^{\frac{5}{2}}}{h^3(4\pi\epsilon n_i)^2}\left(\frac{m_n^*|F_1F_2|^2}{(1+2\mu)\sqrt{1+\mu}}\right)\left(\frac{k_BT}{E_g}\right)^{\frac{3}{2}} \exp\left[-\left(\frac{1+2\mu}{1+\mu}\right)\frac{E_g}{k_BT}\right], \tag{31}$$

where μ is the ratio of conduction to heavy-hole valence band effective mass, ϵ is the permittivity of the material F_1, and F_2 are the overlap integrals of the periodic part of the electron wave functions, with constant practical value of $|F_1F_2|$ between 0.1 and 0.3. Several

authors reported the value of C_{na} in n-type GaSb to be of the order of $10^{-(29\pm1)}$cm^{6}s^{-1}. The value used for the analysis of n-type GaSb in the present work is of the same order as these reported values.

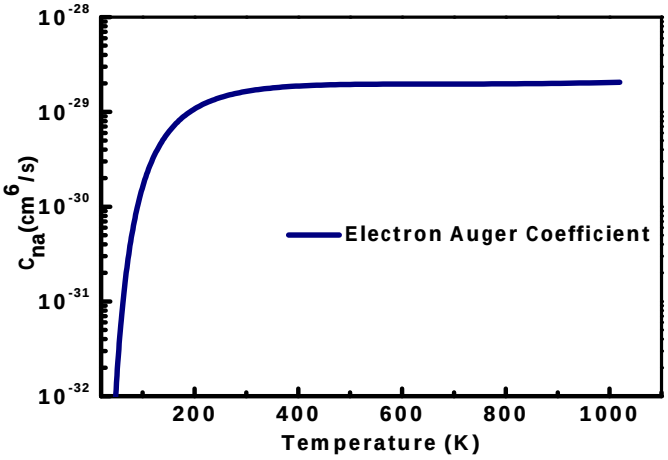

Figure 2-5: Temperature dependence of the Electron Auger recombination coefficient.

Figure 2-5 shows the temperature dependence of the Auger recombination coefficient for the conduction band electron recombines with a heavy hole (C-H) and a conduction electron is excited to a higher energy level (C-C) is described. A maximum Auger recombination coefficient exists, with a strong decrease at low temperatures and a remains constant at higher temperatures above 400 K as shown in figure 2-5. C_{na} is dominant in a small and direct bandgap n-type GaSb [55].

ii. *Hole Auger capture coefficient*

The dominant recombination mechanism in p-type GaSb and other small band gap materials at relatively higher injection level is the band-to-band Auger S (CHHS) process, in which a heavy hole recombines with a conduction band electron (C-H) and a heavy hole is excited to the spin-orbit split off the valence band (H-S). As reported by several authors, the spin-split off valence band plays a far more important role than the light-hole valence band for p-type direct band gap materials, especially when the band gap energy, E_g approaches the spin-orbit splitting, ΔE_{0S}. Benz and Conradt determined a very high CHHS hole capture coefficient of $10^{-(25\pm1)}$cm^{6}s^{-1} by measuring the excitation and doping dependence of the luminescence produced by the recombination of Auger excited holes. The result, however, relied on an estimation of the internal quantum efficiency of the recombination luminescence. Titkov *et*

al. also derived a significantly smaller Auger coefficient of $2.5\times10^{-29}\text{cm}^6\text{s}^{-1}$ for degenerate p-type GaSb using an optical orientation method. The Auger coefficient due to Auger S (CHHS) used in this work is calculated using Haug's formula. Haug reported that, because the values of E_g and the valence band splitting, ΔE_{0S} are nearly equal, Auger recombination due to valence band splitting seems to be favoured in GaSb. The Auger process, which involves the spin-split-off valence band (CHHS), is very efficient, since energy and wave vector conservation allow 'vertical' transitions in *k*-space. The corresponding Auger capture coefficient for holes in the case of non-degenerate carrier densities (Boltzmann statistics) is given by [2, 26]:

$$C_{pa} = \begin{cases} ABx^2e^2\frac{2}{\sqrt{\pi}}\left[\Gamma\left(\frac{5}{2},\mu x\right)\right] - \frac{2\Gamma\left(\frac{7}{2},\mu x\right)}{\mu x} + \frac{\Gamma\left(\frac{9}{2},\mu x\right)}{\mu x}, & \text{for } E_g \geq \Delta E_{0S}, \\ AB\left[\frac{35}{(2\mu x)^2}\right], & \text{for } E_g = \Delta E_{0S}, \\ ABx^2e^2\frac{3}{2}\left[1 - \frac{5}{\mu x} + \frac{35}{(2\mu x)^2}\right], & \text{for } E_g \leq \Delta E_{0S}, \end{cases} \tag{32}$$

where

$$\begin{cases} x = \dfrac{E_g - \Delta E_{0s}}{k_B T}, \quad \mu = \dfrac{2m_P^* + m_C^*}{2m_P^* + m_C^* - m_{S0}^*}, \quad \Gamma(a, x_0) = \displaystyle\int_{x_o}^{\infty} e^{-t}\, t^{a-t} dt \\ A = \dfrac{h^3 e^4}{(2m_n k_\infty)^2}\left(\dfrac{m_P^*}{m_V^*}\right)\left(\dfrac{m_{S0}^*}{2m_P^* + m_C^*}\right)^{\frac{3}{2}}, \quad B = \dfrac{E_p^2\left(1 + \frac{m_{S0}^*}{m_n}\right)}{9E_g^2\,\Delta E_{0S}^2\left(E_g + \Delta E_{0S}\right)}. \end{cases} \tag{33}$$

The parameter $\Gamma(a, x_o)$ is the incomplete gamma function, $m_{c,p,s}^*$ the effective masses of the corresponding bands, m_V the density-of-states mass of the valence band and E_p is the square of the momentum matrix element, multiplied by $2/m_n$ and its value is 22.4eV. The temperature dependence of the valence band split-off energy ΔE_{0S}(eV) is given by Haug as:

$$\Delta E_{S0}(T) = 0.743 + \frac{1.89\times10^{-4}T^2}{T + 94} \tag{34}$$

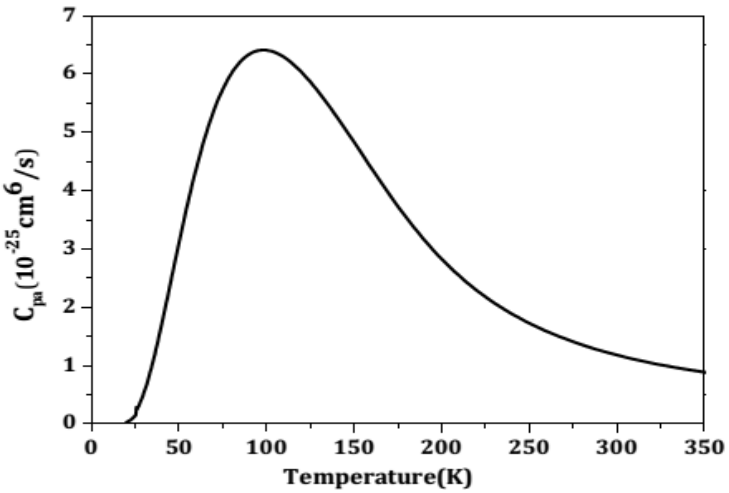

Figure 2-6: Temperature dependence of the Auger recombination coefficient.

Figure 2-6 depicts the temperature dependence of the Auger recombination coefficient for the spin split-off valence band described. According to Haug, a maximum Auger Recombination Coefficient (C_{pa}) exist, decreases strongly for lower temperatures whereas the decrease is weaker for higher temperatures, as shown in this figure. The maximum value of a temperature is approximately at T = 95 K to T = 100K. In particular, the value for room temperature is only about 1/10 of the maximum value. If one chooses f_{CH} = 10 and f_{SH} = 0.1 which is reasonable then the curve gives the value of C_{pa} directly, the higher values of C_{pa}, especially at low temperatures. Not only is the minimum of the gain curve at T = 100K in good agreement with the maximum of the C_{pa} at T = 95 K, but also the general course of the gain curve with a strong increase for low temperatures and a weaker increase for high temperatures corresponds exactly to the Auger curve (figure 2.6) [55]. Since C_{pa} is dominant in p-type GaSb. Next, we wish to evaluate the steady-state description of and for the optically generated excess carriers. If the Auger recombination rate is dominant in the material at steady state, the net recombination rate is equal to the optical generation rate of excess carriers.

Auger recombination is viewed as a three particle interaction where a conduction band electron and a valence band hole recombine, with the excess energy being transferred to a third free electron or hole. The charge carriers involved are assumed to be non-interacting quasi-free particles. The eeh process denotes when the excess energy is transferred to another electron, with the recombination rate given by $U_{eeh} = C_{na}n^2p$. Similarly, the ehh

process denotes when the excess energy is transferred to another hole, with recombination rate $U_{ehh} = C_{pa}p^2n$ [23].

The total recombination mechanism rate and its lifetimes are taken by the following equations. The total Auger recombination rate, R_A is then given by

$$R_A = U_{eeh} + U_{ehh} = C_{na}n^2p + C_{pa}p^2n \tag{35}$$

where p and n are the hole and electron concentrations,

C_{pa} and C_{na} are the hole and electron Auger recombination coefficients. The rate of Auger recombination in thermal equilibrium condition can be written as:

$$R_{th} = G_{th} = C_{na}n_0^2p_0 + C_{pa}p_0^2n_0 \tag{36}$$

$$U_A = R_A - G_{th}$$

G_{th} is the rate of Auger recombination in thermal equilibrium condition, R_A is the total Auger recombination rate, or

$$U_A = C_{pa}\,(p^2n - p_o^2n_o) + C_{na}(n^2p - n_o^2p_o) \tag{37}$$

When inserting,$n = n_o + \delta n,\ p = p_o + \delta p$, into equation (37) and we obtained:

$$U_A = \delta n(C_{pa}(p_0^2 + 2n_i^2) + C_{na}(n_0^2 + 2n_i^2)) + \delta n^2(C_{pa}(2p_0 + n_0) + C_{na}(2n_0 + p_0)) + \delta n^3(C_{pa} + C_{na}) \tag{38}$$

The simplified form of the Auger recombination rate, U_A for photo-generated carrier in Equ. (38) becomes:

$$U_A \approx \frac{\delta n}{\tau_{A0}} + k_A\delta n^2 + C_A\delta n^3 \tag{39}$$

and the Auger recombination lifetime for excess carriers is then given by:

$$\tau_A = \frac{\tau_{A0}}{1 + \tau_{A0}(k_A\delta n + C_A\delta n^2)}, \tag{40}$$

where

$$\tau_{A0} = \frac{1}{C_{pa}(p_0^2 + 2n_i^2) + C_{na}(n_0^2 + 2n_i^2)}, \qquad C_A = C_{pa} + C_{na},$$

$$k_A = C_{pa}(2p_0 + n_0) + C_{na}(2n_0 + p_0).$$

For narrow band gap p-type semiconductors, Auger recombination due to valence band splitting is favored, $C_{pa} \gg C_{na}$, so that, $\tau_{A0} \approx \frac{1}{C_{pa}p_0^2}$, $k_A \approx 2C_{pa}p_0$, and $C_A \approx C_{pa}$.

Next, we wish to evaluate the steady-state description of δn and τ_A for the optically generated excess carriers. If the Auger recombination rate is dominant in the material at

steady state the net recombination rate is equal to the optical generation rate of excess carriers [2]:

$$G_0 \approx U_A \approx \frac{\delta n}{\tau_{A0}} + k_A \delta n^2 + C_A \delta n^3 \tag{41}$$

For high injection levels, the cubic term in the density of the excess carrier on the right side of Eqn. (41) dominates and hence, $G_0 = U_A = C_A \delta n^3$, so that:

$$\delta n \approx \sqrt[3]{\frac{G_0}{C_A}} \text{ and } \tau_A = \frac{\delta n}{G_0} \approx \frac{1}{\sqrt[3]{G_0^2 C_A}}. \tag{42}$$

For low injection levels, the linear term in the density of the excess carrier on the right side of Eqn. (41) dominates, so that $G_0 = U_A = \frac{\delta n}{\tau_{A0}}$ and hence:

$$\delta n \approx G_0 \tau_{A0} \text{ and } \tau_A \approx \frac{\delta n}{G_0} = \tau_{A0}. \tag{43}$$

The effective lifetime for both recombination mechanisms in the simplified form of the well-known radiative (τ_R) and Auger (τ_A) excess carrier recombination lifetimes are described in terms of the thermal equilibrium carrier concentration p_o and δn for p-type bulk material as [11]. From the combination of equation (28) and (40), we obtained as follows:

$$\frac{1}{\tau_{\text{eff}}} = \frac{1}{\tau_R} + \frac{1}{\tau_A} \quad \text{or} \quad \tau_{\text{eff}} = \left(\frac{1}{\tau_R} + \frac{1}{\tau_A}\right)^{-1}. \tag{44}$$

Impact ionization refers to the transfer of mechanical energy of a charge carrier (electron or hole) to another similar fixed charge carrier that is initially attached to an atom in the material. Upon this interaction the charge carrier that receives mechanical energy started to move freely in the material and the charge carrier that transfers mechanical energy to it is recombined with another free opposite charge carrier. Recombination refers to any process whereby any electron is captured by a free hole and both of them stopped the conduction process. Electron has not been vanished in the process of recombination; it remains attached to the atom in the valence band again until it becomes free by another ionization process. When holes and electrons are separated by any ionization mechanism and started to move freely in the material, we say free or excess carriers are generated. For each generation process there is an inverse recombination process [65].

Chapter 3

Methodology

The primary task of this work was to select the model of a semiconductor sample. Gallium antimonide (GaSb) was found to be suitable for its small and direct bandgap and its very high purity. The majority carrier concentration, p_0 used in the analysis for different doping levels GaSb samples was taken from the simulation of the existing temperature dependence Hall measurements data measured at Nelson Mandela Metropolitan University, South Africa. The minority carrier concentration, n_0 is determined from p_0 using the law of mass action for a particular semiconductor using relation Eqn. (9). The dopant concentrations can be determined for samples with different doping levels using the complete ionization temperature region in which the donor or the acceptor impurities are dominant in contributing the free carriers as simulated in figure 2.3 (b) above. The Fermi energy for samples with different doping levels can be determined using the free carrier concentrations from the relation in Eqn. (12).

The effective excess carrier lifetime was determined using the two recombination mechanisms radiative and Auger that are usually dominant in small band gap materials. The radiative lifetime (τ_R) and Auger lifetime (τ_A) for excess carriers in p-type GaSb material are determined as functions of doping, temperature and injection level. The theoretical results were analyzed using the thermal equilibrium majority carrier concentration results from Hall Effect measurements along with the relations describing the effective excess carrier lifetimes in the bulk of direct band gap semiconductor. First, the data for τ_{eff} was described using Eqn. (44) along with Eqns. (28) and

(40) in all the cases. The results of the analyses were described using semi-log graphs for all the excess carrier lifetimes.

The results of the doping dependence of the room temperature effective carrier lifetime(τ_{eff}) were described using the combinations of Eqns. (44), (28) and (40) by varying the doping level from intrinsic to highly doped samples. The analysis for this data was performed using semi-log for both the effective excess carrier lifetime and the doping level axes. The values of the excess carrier lifetimes in this case is varied from 10^{-5} ns to 10^{10} ns.

The description of the results of the temperature dependence of the excess carrier lifetimes were also performed by varying the temperature ranges from 20 K to 1000 K for fives samples with different doping levels. That is, N_a = $0, 10^{12}\text{cm}^{-3}, 4.7\times10^{14}\text{cm}^{-3}, 10^{16}\text{cm}^{-3}$ and , 10^{19}cm^{-3}. In the analysis of this result, the vertical axis for the effective excess carrier lifetime was taken as semi-log and the horizontal axis of the temperature was kept linear. The results obtained for the excess carrier lifetimes for all the doping levels were varied from 10^{-6} ns to 10^{13} ns.

For the description of the injection level dependence of the excess carrier lifetime, again four samples with doping levels, N_a = $0, 4.7\times10^{14}\text{cm}^{-3}, 10^{17}\text{cm}^{-3}$ and , 10^{19}cm^{-3}. The analysis for this data was performed using semi-log for both the effective excess carrier lifetimes and the axis of free carrier injection level, by varying the free carrier injection levels ranges from $10^{8}\text{cm}^{-3}$to 10^{19}cm^{-3}. The results obtained for the excess carrier lifetimes for all the injection levels were varied from high injection level value, 10^{-6} ns to the low injection value to 10^{10} ns.

Chapter 4

Analysis of Data and Discussion

In this section, the description of the impact ionization and optical generation of free charge carriers is presented in detail for GaSb samples with different doping level at different temperature and injection levels. Since the minority carrier lifetime plays determinant role in the performance of a given semiconductor, the description of the effective excess carriers lifetime, τ_{eff} for the minority carrier lifetime sufficient for the analysis this work. The values of τ_{eff} described under different conditions in this work are all determined using Eqns. (44), (28) and (40) from the combined effects of the radiative and Auger excess carrier lifetimes, τ_R and τ_A, respectively.

4.1 Doping level dependence of excess carrier lifetime

Figure 4.1 illustrates the room temperature doping concentration dependence of excess carrier lifetime for p-type semiconductor under low injection level as predicted by Equation (44) from intrinsic level to high doping level. The determination of the doping level dependence of effective excess carriers' lifetime, τ_{eff} in this case is performed from the analysis of Eqn. (44) at low injection level.

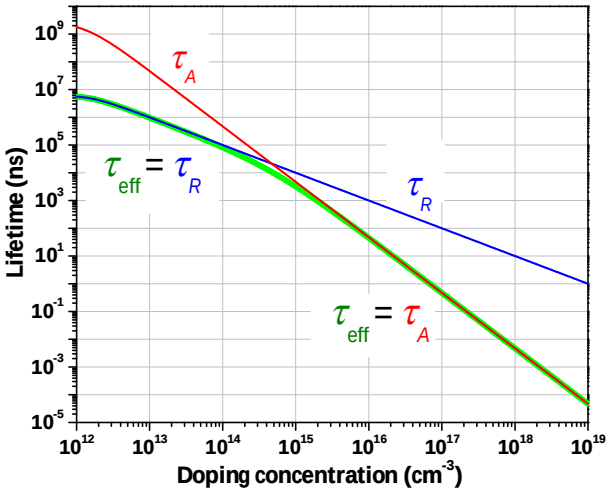

Figure 4-1: Doping level dependence of excess carriers' lifetime at low injection level ($\delta n \ll p_0$).

To perform the process of plotting the graph in figure 4.1, first the doping level dependence of τ_{eff} was described using Eqn. (44) at low injection level ($\delta n \ll p_0$). As can be seen from the relations in Eqns. (28) and (40), the excess carrier lifetime has inverse proportion with the doping concentration for both the radiative and the Auger case. The radiative excess carrier lifetime varies approximately from 1 millisecond at intrinsic level to 10 nanoseconds for highly doped samples. The result obtained is in complete agreement with the result obtained as that of Ascazubi *et al*. [68]. According to Ascazubi, the Auger excess carrier lifetime varies

approximately from 1 second at intrinsic level to 0.1 picosecond for highly doped samples. Titkov *et al.* also determined the similar result for Auger excess carrier lifetime [67]. The Auger recombination mechanism is hence the dominant mode of recombination at high doping levels, approximately above the doping level of $4.7\times10^{14}\text{cm}^{-3}$. Nevertheless, the radiative recombination which is lightly affected by doping level as compared to the Auger recombination is dominant at very low doping regime. The effective excess carrier lifetime is hence decreases slightly at a slower rate in the low doping region and at a faster rate in the higher doping regime as shown in Figure 4.1, because of the styles of the variation of the two involved mechanisms with the doping concentration.

It is known that, radiative recombination mechanism is the inverse of optical generation of electron-hole pairs in the conduction and valence bands, whereas band to band Auger recombination mechanism is the inverse of band to band impact ionization process, in which an energetic carrier causes electron-hole pair generation. These reversed processes were balanced in both cases under the condition of detailed balance or at steady state condition. Therefore, the graph in Figure 4.1 shows clearly, the effects of optical generation of free carriers and the impact ionization with relation to the doping level of the semiconductor at low injection level.

Therefore, one can conclude from these relations that, the optical generation of excess carriers dominates the low doping level and the impact ionization dominates the higher doping regime.

4.2 Temperature dependence of excess carrier lifetime

Figure 4.2 depicts the temperature dependence of excess carrier lifetimes for (a) intrinsic samples; and for samples with acceptor density equal to (b) 10^{12}cm^{-3}, (c) $4.7\times10^{14}\ \text{cm}^{-3}$, (d)$10^{16}\ \text{cm}^{-3}$ and (e) 10^{19}cm^{-3}. The radiative excess carrier lifetimes are represented by blue lines, the Auger excess carrier lifetimes are represented by red lines and the effective excess carrier lifetimes are represented by green lines. As can be seen from Figure 4.2, the style of the variation of the excess carrier lifetime with temperature also depends on the doping level of the semiconductor.

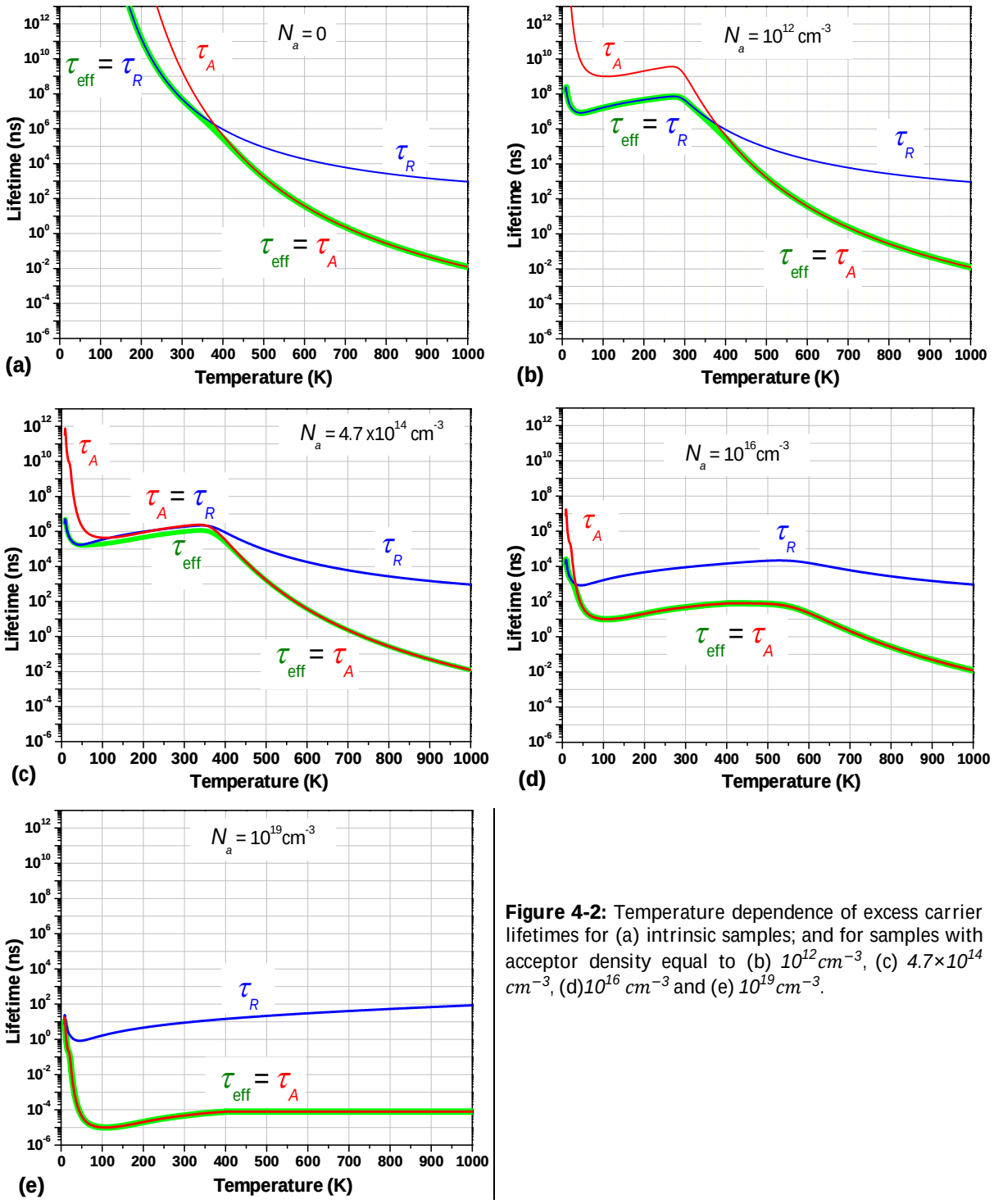

Figure 4-2: Temperature dependence of excess carrier lifetimes for (a) intrinsic samples; and for samples with acceptor density equal to (b) $10^{12} cm^{-3}$, (c) 4.7×10^{14} cm^{-3}, (d)10^{16} cm^{-3} and (e) $10^{19} cm^{-3}$.

The functional dependence of the lifetime on temperature shown in Figure 4.2 is predicted by Eqn. (44), when considered along with the temperature dependences of the capture coefficients, Eqns. (25), (31) and (32); and the temperature dependences of the

thermal equilibrium carrier concentrations, simulated from the Hall measurement results of gallium antimonide (GaSb) samples as in figure 2.3 for samples with different doping levels.

At very low temperature, in the partial ionization region (below 100 K), both the radiative and Auger excess carrier lifetimes are highly intensified with decreasing temperature, because of the freeze out of charge carriers in the respective bands and hence the decrease in the recombination processes.

In the completely ionization region, both the radiative and the Auger excess carrier lifetimes increase slightly up to the extrinsic region because of the fixed values of the majority carrier concentrations and the decrease in both the radiative and the Auger hole capture coefficients. The complete ionization region is getting wider and wider with increasing temperature, because of the variation of the carrier concentration in this region as function of doping (see figure 4.2). This is not observed in the photo response of a sample without acceptor or donor concentration as can be seen in figure 4.2 (a). The region varies approximately from 100 K to 230 K for samples with acceptor concentration equal to 10^{12} cm^{-3}(see figure 4.2 (b)), from 100 K to 450 K for samples with acceptor concentration equal to 4.7×10^{14} cm^{-3}(see figure 4.2 (c)), from 100 K to 500 K for samples with acceptor concentration equal to 10^{16} cm^{-3} (see figure 4.2 (d)) and from 100 K to above 1000 K for samples with acceptor concentration equal to 10^{19} cm^{-3}(see figure 4.2 (e)).

In the intrinsic region, both the radiative and the Auger excess carrier lifetimes decrease slightly with increasing temperature irrespective of the doping effect with the Auger recombination mechanism as the dominant recombination mechanism. This is because of the highly increasing of the intrinsic carrier concentration with increasing temperature and the intrinsic carrier concentration is in general very high at very high temperature. As one can see from figure 4.2, hence, the optical generation rate is dominant in lower doping samples at lower temperature range and impact ionization is dominant in highly doped samples at higher temperature ranges in all the samples.

As a result, the value of the bulk effective excess carrier lifetime in this case is rising–up in the partially ionization region with decreasing temperature, slightly increasing in the complete ionization region and slightly decreasing regardless of the acceptor concentration in the intrinsic regions of all the samples.

4.3 Injection level dependence of excess carrier lifetime

In general, photo-generated carriers can be recombined both with opposite photo-generated carriers and thermally-generated carriers in the material. Each of the recombination rate for photo-generated carriers discussed above is hence the sum of the recombination rate of a photo-generated carrier with opposite photo-generated carriers and thermally-generated carriers. The net recombination rate of photo-generated carriers with other photo-generated carriers is dominant in high injection level material, while the net recombination rate of a photo-generated carrier with the thermally generated carriers is dominant in low injection level material. As a result, the excess carrier lifetimes given in Eqns. (28), (40) and (44) remain only a function of photo-generated carrier concentrations in high injection level system and only a function of thermally-generated carrier concentrations in low injection level materials.

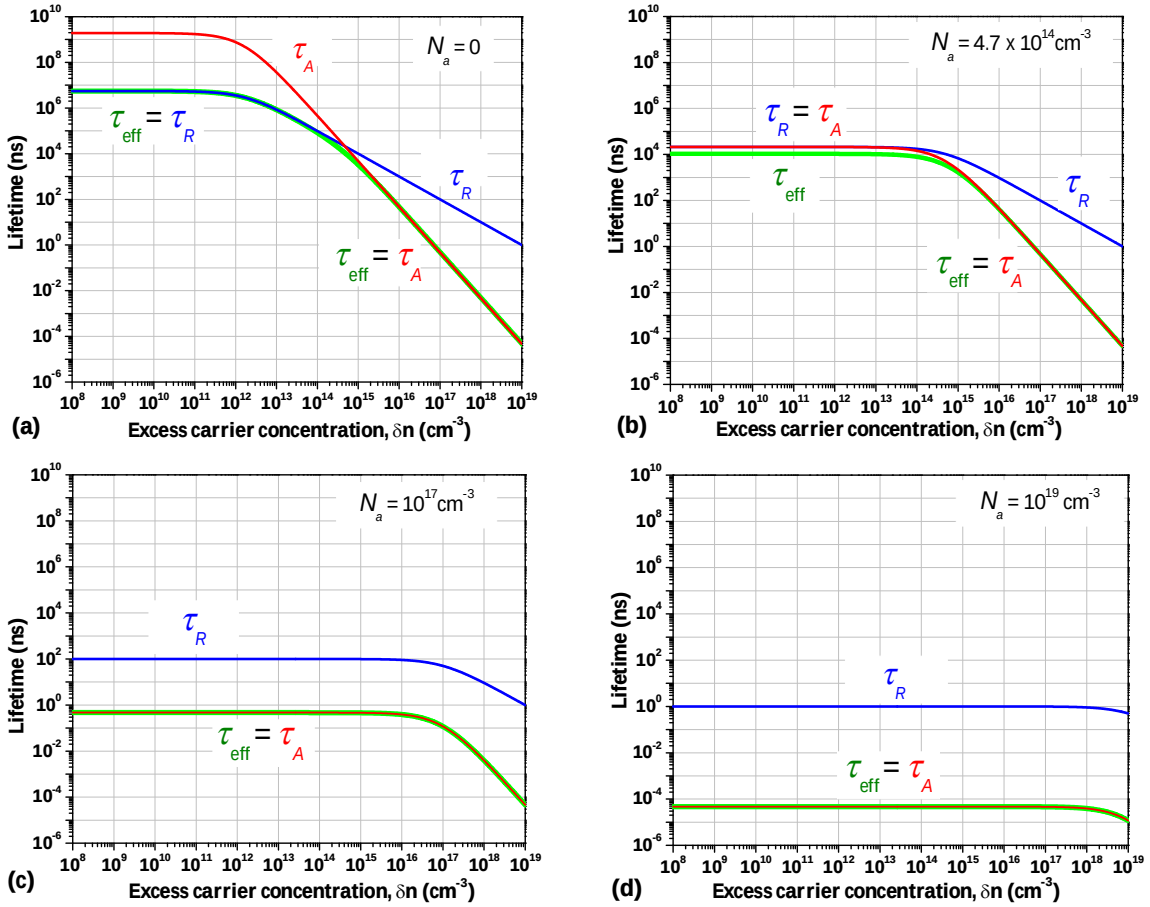

Figure 4-3: Injection level dependence of excess carrier lifetimes for (a) intrinsic samples; and for samples with acceptor density equal to (b) $4.7\times10^{14}\ cm^{-3}$, (c)$10^{17}\ cm^{-3}$ and (d) $10^{19} cm^{-3}$.

The description of the injection level dependence of the excess carrier lifetimes can be predicted by varying the photo-generated carriers in relations (28), (40) or (44). Figure 4.3 depicts the injection level dependence of excess carriers' lifetimes for p-type samples. In all the samples in Figure 4.3, both the radiative and the Auger excess carrier lifetimes remain constant at low injection level ($\delta n \ll p_0$) and decrease in the high injection regime ($\delta n \gg p_0$). The radiative excess carrier lifetime is dominant at low injection level in a sample of very low acceptor or donor concentration (see figure 4.3 (a)). The Auger excess carrier lifetime is dominant at low injection level in a sample of relatively high acceptor or donor concentration as shown in figure 4.3 (b), (c) and (d) and dominant at high injection level in all the samples in the high injection level samples irrespective of the acceptor or donor concentrations as shown in all the graphs in figure 4.3. This is because of most of the photo-generated carriers are involved in the process of generating electron-hole pairs (impact ionization) rather than giving off photons during their recombination with the opposite charge carriers.

Depending on the dominance of the doping level or the injection level, the region under the curve of the excess carrier lifetime in figure 4.3 can be divided in two. The first regions where the excess carrier lifetimes remain constant with increasing the injection level in all the samples are the region where the thermal equilibrium majority carriers dominate the entire recombination mechanism ($p_0 > \delta n$). This condition is called *low injection level*. The regions where the excess carrier lifetimes decrease with increasing the injection level are where the injection levels dominate the entire recombination mechanism ($\delta n > p_0$), and this condition is called *high injection level.*

As can be seen from figures 4.1 to 4.3 above, the effective excess carrier lifetime decreases slightly at a slower rate in the low doping region where radiative recombination is dominating the entire process and at a faster rate in the higher doping regime where Auger recombination is dominating the entire process.

Chapter 5

Conclusions

In this study, the effects of the photo-response of gallium antimonide (GaSb) by describing the doping level, the temperature dependence and as well as the injection level dependences the excess carrier lifetimes. The effective excess carrier lifetimes for minority carriers in the entire bulk of a given sample was calculated from the combined effects of the radiative and Auger recombination mechanisms. The room temperature doping level dependence results of the excess carrier lifetime revealed that, the main contribution of the photo-response comes from the radiative recombination mechanism at very low doping level and from Auger recombination mechanism at very high doping level. As a result, the room temperature values of the low injection level minority carrier lifetimes in GaSb varies approximately from 0.1 picoseconds for highly doped samples to 1 second for intrinsic samples. As the temperature of the sample increases, additional electron-hole pairs are thermally generated by thermal ionization of donors or acceptors, so that, the carriers generated by the ionization of donors or acceptors starts to dominate the entire conduction process in the partial ionization region. When the temperature is increased beyond the partial ionization region, the acceptor level is completely ionized and the carrier concentration remains constant. In the completely ionization region, both the radiative and the Auger excess carrier lifetimes remain constant slightly with increasing temperature irrespective of the doping effect with the Auger recombination mechanism as the dominant recombination mechanism in the region for highly doped samples. The radiative recombination mechanism also dominates in the region for the un-doped and slightly doped samples. The entire intrinsic region is dominated by the Auger recombination mechanism because of the highly increasing of the intrinsic carrier concentration above the dopant concentration with increasing temperature. The room temperature injection level dependence of the excess carrier lifetimes also shows that radiative recombination mechanism dominates the low injection level in the un-doped or slightly doped samples and Auger recombination mechanism dominates the entire injection level in highly doped samples. Finally, one can conclude from the obtained results that, variations of the effective excess carrier lifetimes with doping, temperature and injection levels is slower in the region

where the radiative mechanism is dominating the entire recombination process and faster in the region where Auger mechanism is dominating the entire recombination process.

References

[1] J. B. R.J. Kumar, "Journal of Applied Physics," 2005.

[2] M. W. Shura, V. Wagener, J. R. Botha and M. C. Wagener, *Non-linear injection level dependence of the excess carrier lifetime of p-type GaSb thin films*: A two-layer model, J. Appl. Phys. 111 (2012) 113104.

[3] S. S. Li, Semiconductor Physical Electronics, Second Edition, 2006.

[4] A. B. O.V. Sulima, Fabrication and simulation of GaSb thermo-photovoltaic cells, 2001.

[5] Barnbas Achakpa Ikyo, "Electron-Hole and Photon Recombination Processes in Quantum Well Semiconductor Lasers," Journal of Optics and Photonics, 2015.

[6] R. a. S. Brian r. Bennett, "journal of quantum electronics," vol. 26, 1990.

[7] L. W. BridEman, Hall Effect "The thermodynamics of Electrical Phenomena in Metals, 1934.

[8] B. K. Ridley, Tr. J. of Physics; Large-Band-gap Semiconductors, 1999.

[9] B. R. Green, Hall Effect measurement for Semiconductors and material characterization, 2011.

[10]]. M. S. Dresselhaus, Optical Properties of Solids, 1975.

[11] M.W. Shura, V. Wagener, M. C. Wagener, J. R. Botha, Physica B 407, *Photoconduction spectroscopy of p-type GaSb films*, 2012.

[12] R. P. a. P. S. D. A Chandola, below band-gap optical absorption in tellurium-doped GaSb, 2005.

[13] R. Ascazubi, The Emission Spectroscopy of narrow band-gap semiconductors, 2005.

[14] C.-W. H. Y.-Y. T. a. W.-C. L. Po-Hsien Lai, Temperature effect on impact ionization characteristics in metamorphic high electron mobility transistors, 2006.

[15] R. Green, Hall Effect measurement for Semiconductors and material characterization, 2011.

[16] A. Rogalski, Auger processes HgCdTe infrared detector material, 2005.

[17] P. T. L. a. A. F. W. Willoughby, Proceeding of the International Conference on Recombination Mechanisms in Semiconductors, in Solid State Electronics, 1978.

[18] M. G. a. E. B. Francesco Bertazzi, Auger Lifetime in Narrow Gap Semiconductors, 2007.

[19] L. M. K. Pattie, Acceptor Defects in p-type Gallium Antimonide Materials, 2005.

[20] J. Piotrowski, Infrared Detectors, 1995.

[21] M. M. A.V. Dmitrie, Recombination and ionization in narrow gap semiconductors, 1995.

[22] M. J. Kerr, Surface, Emitter and Bulk Recombination in Silicon andDevelopment of Silicon Nitride Passivated Solar Cells, 2002 .

[23] B. V. Zeghbroeck, Principles of Semiconductor Devices, 2002.

[24] J. F. Roller, Contactless Spectral-Dependent Measurement of Bulk Lifetime and Surface Recombination Velocity in silicon photovoltaic materials, 2016.

[25] Y. D. M. D. Ö. H. T. Koçer, Simulation of Performance Parameters of Mercury Cadmium Telluride Infrared Photodetectors Hasan, 2012.

[26] B. G. S. a. S. K. Banerjee, Solid state Electronic Devices, 2009.

[27] M. Z. Rahman, Modeling Minority Carrier's Recombination Lifetime of p-Si Solar Cell, (2012.

[28] L. M. K. Pattie, Acceptor Defects in p-type GaSb Materials, 2005.

[29] B. V. Zeghbroeck, Semiconductor Fundamentals, 2011.

[30] N. Barishev, Band-to-band recombination of electrons and holes in indium arsenide, 1964.

[31] A. Beattie, Quantum Efficiency in InSb, J. Phys.Chem. Solids, 1962.

[32] A. &. L. Beattie, P.T. Auger effect in semiconductors, 1959.

[33] W. Lochmann, Phonon-Assisted Auger Recombination in Semiconductors. Phys. Status Solid., 1997.

[34] M. Takeshima, Simple Method of Calculating Phonon-Assisted Auger Recombination Rate in Direct-Gap Semiconductors. Jpn. J. Appl. Phys., 1983.

[35] A. Haug, Auger Recombination in Direct-Gap Semiconductors: Band-Structure Effects. J. Phys. C: Solid State Phys., 1983.

[36] S. Picozzi, R. Asahi, C. B. Geller and A. J. Freeman, Accurate First Principles Detailed-alance Determination of Auger Recombination and Impact Ionization Rates in Semiconductors. Phys. Rev. Lett, 2002.

[37] B. A. &. H. M. C. Gregg, Comparing organic to inorganic photovoltaic cells: Theory, experiment, and simulation. J. Appl. Phys, 2003.
[38] X. D. G. N. M. A. J. S. v. d. Z. A. M. &. M. P. L. Xu, Photo thermoelectric effect at a graphene interface junction. Nano. Lett., 2010.
[39] M. e. a. Buscema, Large and tunable photo thermoelectric effect in single-layer MoS2. Nano. Lett., 2013.
[40] G. B. a. R. Conradt, Auger Recombination in GaAs and GaSb, 1976.
[41] R. N. Hall., Recombination Processes in Semiconductors, 1959.
[42] R. Braunstein, Radiative Transitions in Semiconductors', Physical Review, 1955.
[43] T. S. a. H. T. H. Moss, Recombination Radiation from InSb, 1956.
[44] C. Z. a. D. N. D. Van Doorn, Luminescence, Transmission, and Energy Gap of CdTe Single Crystals', Physica,, 1956.
[45] D. H. Clarke, Semiconductor Lifetime as a Function of Recombination state density, 1957.
[46] S. G. Kalashnikov, Studies of the Recombination of Electrons and Holes in Germanium, 1959.
[47] Jasprit Singh, Electronic and Optoelectronic properties of Semiconductor Structures, 2003.
[48] M. Bernard, Recombination at Two-Level Impurities in Semiconductor, 1958.
[49] M. C. T. J. W. Bahaa E. A. Saleh, Photons in Semiconductors, 1991.
[50] M. Z. Rahman, Modeling Minority Carrier's Recombination Lifetime of p-Si Solar Cell, Dhaka 1208, Bangladesh, 2011.
[51] J. F. Roller, Contactless Spectral-Dependent Measurement of Bulk Lifetime and Surface Recombination Velocity in Silicon Photovoltaic Materials, University of Maryland, 2016.
[52] J. M. B. P. S. D. R. J. G. C. A. W. e. a. (R. J. Kumar, Auger and radiative recombination coefficients in 0.55-eV InGaAsSb, Journal of Applied Physics, 2003.
[53] Z. R. Michal Pokorný, Modeling of Microwave Semiconductor Diodes, 2008.
[54] S. W. a. D. Macdonald, Temperature dependence of Auger recombination in highly injected crystalline silicon, J. Appl. Phys., 2012.
[55] A Haugt, Temperature dependence of Auger recombination in gallium antimonide, Federal Republic of Germany, 1984.
[56] Q. Y. D. S. a. C. G. V. d. W. Emmanouil Kioupakis, Temperature and carrier-density dependence of Auger and radiative recombination in nitride optoelectronic devices, New J. Phys., University of California, 2013.
[57] B. G. S. a. S. K. Banerjee, Solid state Electronic Devices, 2009.
[58] B. G. Streetman, In Solid state electronic devices', 3rd. ed. Prentice Hall, Inc, Englewood cliffs, N.J, U.S.A., 1990.
[59] W. K. a. J. Luttinger, " Phys. Rev.," vol. B8, p. 915, 1955.
[60] P. G. i. a. J. P. P.M. Fahay, " Rev. Mod. Phys.," vol. 81, p. 385, 1989.
[61] C. Sah, " Solid State Electron," vol. 19, p. 975, 1976.
[62] G. H. L. a. H. H. w. bury, " Solid State Phys.," vol. 13, p. 223, 1962.
[63] F. B. L. H. J. Bardeen, "Indirect transitions from the valance to the conduction bands, Photoconductivity Conference, Atlantic City,," pp. ,pp. 146-154, 1954.
[64] P. C. R.K. Lal, A comparison of dominant recombination mechanisms in n-type InAsSb materials, Banaras Hindu University, India, 2006.
[65] E. S. S. Bremner, ELEG620: Solar Electric Systems, University of Delaware, 2009.
[66] D. K. Schroder, Carrier Lifetimes in Silicon, IEEE Transactions on electron devices, vol. 44, No. 1, 1997
[67] A.N. Titkov, G.V. Benemanskaya, and G.N. Iluridze, Scale time for interband Auger recombination involving aspin-orbit-split valance band p-type GaSb crystals, 1981
[68] Ricardo Ascazubi, The Emission Spectroscopy of Narrow band-gap Semiconductors, New York, 2005